Regularization of UV-Divergence for Tidal Conversion Calculations

Norbert Schorghofer
University of Hawaii, Honolulu, HI 96822

April 24, 2011

Abstract

Seamounts in the deep ocean scatter a substantial amount of tidal energy into internal gravity waves. The classic "weak topography approximation" (WTA) provides quantitative estimates for the tidal conversion, but even the smallest discontinuity in the topography leads to an infinite result. Here we analyze this singular perturbation expansion and identify the intrinsic length-scale of the singularity. The energy flux from a thin vertical barrier has singularities of the form $1/\sqrt{x}$, where x is the distance from the discontinuity. The length-scale of the divergent contribution spans exactly the width of topography shadowed by the wave beam. A modification to the WTA is proposed that makes it insensitive to small-scale topographic roughness, leading to robustness and increased accuracy even for continuous topography. An appropriately defined local energy flux is replaced at shadowed segments of the topography with an upper bound that is motivated by the solution for a thin vertical barrier and that depends on topographic relief. When applied to a sample of seafloor topography, the WTA diverges logarithmically with horizontal resolution whereas the regularized WTA does not.

1 Introduction

The generation of internal gravity waves at seamounts in the deep ocean involves a significant fraction of Earth's tidal energy budget, on the order of 1 TW [1, 2]. It has been recognized that the conversion rate calculated with linear wave theory and measured seafloor topography is resolution-dependent [2, 3]. The classical "weak topography approximation" (WTA) is oversensitive to small-scale topographic roughness. One of several pathologies of the approximation is that it diverges for even the smallest discontinuity in the topography. Here we analyze the singular perturbation expansion, identify the nature of the singularity, and use this insight to improve the accuracy of the approximation for continuous topographies. A numerical example using a transect of the mid-atlantic ridge illustrates the success of the regularization.

In brief, the strategy of this paper is as follows. The wavefield is the solution to a linear two-dimensional hyperbolic partial differential equation. The wavefield can have singularities along a discontinuity. For the infinite-order solution the singularity is integrable and does not present a problem, but the infinite-order solution is rarely available. For the commonly used low-order solution (the WTA), the singularity is no longer integrable. The strategy here is to determine the width of the singularity in one relevant case where the infinite-order solution can be obtained analytically and use this width to eliminate the infinite contribution from the WTA. This cures the divergence of the WTA and, more generally, it improves the accuracy of the WTA even when the singularity is not fully developed. The technical parts of the calculation are moved into the appendix while the conceptional parts are in the main text.

In a stratified ocean, water parcels can oscillate vertically due to buoyancy and the barotropic tide causes horizontal motion. The internal gravity wave equation [4, 5] is based on the linearized equations for an inviscid, vertically stratified and rotating fluid. The flow in the plane perpendicular to a ridge is described by a two-dimensional streamfunction, with x the horizontal distance from the center of the ridge and z the vertical distance above the seafloor. The barotropic tide is represented as a spatially uniform oscillatory background flow with horizontal velocity amplitude U_0 and angular frequency ω. The governing equation for the complex-valued streamfunction $\varphi(x,z)$ is [5]

$$\mu^2 \frac{\partial^2 \varphi}{\partial x^2} = \frac{\partial^2 \varphi}{\partial z^2} \tag{1}$$

with

$$\mu = \frac{N_b}{\sqrt{\omega^2 - f_c^2}} \tag{2}$$

Here, N_b is the buoyancy frequency and f_c is the latitude-dependent Coriolis parameter. The characteristics of the solution to (1) are at a slope of $\pm 1/\mu$ relative to the horizontal, which defines a "critical" slope. At the bottom of the ocean, the velocity is tangential to the topography

$h(x)$. An outward radiation condition is used as upper boundary condition.

1.1 Weak topography approximation (WTA)

A solution for small slopes ("weak topography") has long been obtained by Bell [6], assuming that all topographic slopes are negligible compared to the critical slope (or, equivalently, that the critical slope is infinite, $\mu = 0$). The power conversion is [6]

$$P_{\rm WTA} = C \int_0^\infty dk\, k |\tilde{h}(k)|^2 \tag{3}$$

with

$$C = \frac{\rho_0 U_0^2}{2\pi} N_b \sqrt{1 - \frac{f_c^2}{\omega^2}} \tag{4}$$

where k is the wavenumber, $\tilde{h}$ is the Fourier transform of h, and ρ_0 is the density of water.

1.2 The divergence problem

$P_{\rm WTA}$ can be dominated by small-scale topographic roughness. A step discontinuity produces Fourier coefficients that decay proportionally to $1/k$, hence (3) diverges logarithmically at high wavenumber (UV). Thus, for a topography with a discontinuity,

$$P_{\rm WTA} = \infty \tag{5}$$

The "knife-edge" topography is an infinitely narrow barrier of height B. The power conversion of the knife-edge has been obtained analytically, without making the WTA, and it is finite [7, 8],

$$P = \frac{\pi^2}{2} C B^2 \tag{6}$$

For discontinuous topographies, the perturbation expansion in slope (or equivalently in μ) is thus singular,

$$0 \le P = P_{\rm WTA} + \mu^2 P_2 + \mu^4 P_4 + ... < \infty \tag{7}$$

The divergence in the WTA must be compensated by divergencies in the higher orders. When the topography is discontinuous the WTA ($\mu = 0$) no longer corresponds to the limit $\mu \to 0$.

A possible approach to the divergence problem is to use the second order perturbation term P_2 to understand how the logarithmic divergence is canceled, and then use this insight to cure the weak-topography formula. However, the second-order correction requires an even steeper spectral slope for convergence than the weak topography formula [5], and cancellations have not been recognized. Here, the shape of the singularity in an infinite order solution is used to find out how the divergence in the WTA is compensated.

Several physical processes, such as a bottom boundary layer, nonlinearities, an advective component to the flow, or small tidal amplitude can smooth the divergence. However, this only circumvents an intrinsic and interesting mathematical problem. Based on (5) and (7), it must be possible to cure the divergence within the model system (1), without additional physics. In any case, evaluations of the power conversion in the global ocean ultimately use the WTA [e.g., 2, 3].

The tidal-amplitude effect is particularly simple to quantify [6].

$$P = 2\rho_0 \omega^2 N_b \sqrt{\omega^2 - f_c^2} \int_0^\infty dk \frac{1}{k} |\hat{h}(k)|^2 J_1^2 \left(\frac{k U_0}{\omega} \right) \tag{8}$$

For small argument, the Bessel function $J_1(\zeta) \to \zeta/2$, and thus the expression converges and has a cutoff length-scale of $k_c \sim \omega/U_0$. For $U_0 = 0.1$ m/s, $k_c \approx 0.7$ km.

The goal pursued here is to derive an expression for the power conversion that is insensitive to small-scale topographic roughness. Natural topographies are usually characterized by increased roughness at smaller scales. It can be hypothesized that an expression for the power conversion that is free from an unphysical dependence on horizontal spatial resolution must yield a finite power conversion for a discontinuous topography. Solving the divergence problem leads to more accurate and robust results even for rough topographies that are continuous.

2 The Energy Flux

Here we use the simplest possible system that brings out this effect.

2.1 General expressions

The time-averaged vertical energy flux is [5]

$$J(x,z) = \frac{\rho_0 U_0^2}{2\omega} (\omega^2 - f_c^2) \Im(\varphi^* \varphi_z) = \frac{\pi C}{\mu} \Im(\varphi^* \varphi_z) \tag{9}$$

The asterisk (*) indicates complex conjugation. The total power conversion is the total upward energy flux

$$P = \int_{-\infty}^{\infty} dx J(x,z) \tag{10}$$

The WTA solution can be obtained with a Hilbert transform,

$$\hat{H}[h](\zeta) := P.V. \int_{-x_0}^{x_0} dx \frac{h(x)}{x - \zeta} \tag{11}$$

where $P.V.$ denotes the principal value. The streamfunction is [9, 10],

$$\varphi_{\rm WTA}(x,z) \quad = \quad \frac{1}{2} \left(\hat{I} + \frac{i}{\pi} \hat{H} \right) [h](x + \mu z) +$$

$$+\frac{1}{2}\left(\hat{I}-\frac{i}{\pi}\hat{H}\right)[h](x-\mu z) \quad (12)$$

where $\hat{I}$ is the identity operator.

Equations (9) and (12) lead to a general expression for the vertical energy flux $J_{\rm WTA}$. When integrated over all x [10]

$$P_{\rm WTA} = -C\int_{-\infty}^{\infty} dx h(x)\hat{H}'[h](x) \quad (13)$$

$$= +C\int_{-\infty}^{\infty} dx h'(x)\hat{H}[h](x) \quad (14)$$

for any height z, but the integrand does generally not correspond to the energy flux $J_{\rm WTA}$. The prime indicates differentiation. The Hilbert transform is anti-self adjoint and commutes with differentiation [11]. Equations (3), (13), and (14) are three alternative forms for the WTA.

The expression for $J_{\rm WTA}$ simplifies in two limits. One is for an isolated topography in the limit $z\to\infty$, where the two wave beams emanating from an isolated seamount decouple, and

$$J_{\rm WTA}(x>0,z) = \frac{C}{4}\Big[-h(x-\mu z)\hat{H}'[h](x-\mu z) + h'(x-\mu z)\hat{H}[h](x-\mu z)\Big] \quad (15)$$

Partial integration of one of the two terms in the square bracket shows that both terms contribute equally to the total power conversion.

An even simpler expression for the energy flux is obtained from (9) and (12) for $z=0$,

$$J_{\rm WTA}(x,0) = -Ch(x)\hat{H}'[h](x) \quad (16)$$

Equation (16) shows that the integrand in (13) can be interpreted as the vertical energy flux at zero height, irrespective of the fact that the topography extends beyond this height. Moreover, this integrand has the same shape as the first of the two terms on the right-hand side of (15). The association of $J_{\rm WTA}(x,0)$ with the integrand in (13) greatly aids our considerations, because we can work with the one-dimensional function (16) instead of the general expression for $J(x,z)$.

2.2 Rectangular topography in WTA

A rectangular topography is described by $h(x)=B$ for $|x|\le x_0$ and $h(x)=0$ otherwise. The knife-edge topography is obtained in the limit $x_0\to 0$. The Hilbert transform (11) is

$$\hat{H}(\zeta) = B\ln\left|\frac{\zeta-x_0}{x_0+\zeta}\right| \quad (17)$$

The first term in the energy flux (15) vanishes outside the two intervals $|x\pm\mu z|<x_0$. Inside this interval,

$$-h(x-\mu z)\hat{H}'(x-\mu z) = B^2\left(\frac{1}{x-\mu z+x_0}-\frac{1}{x-\mu z-x_0}\right) \quad (18)$$

The second term in (15) is

$$h'(x-\mu z)\hat{H}(x-\mu z) = B^2\left[\delta(x-\mu z-x_0) - \delta(x-\mu z+x_0)\right]\ln\left|\frac{x^2-(x_0-\mu z)^2}{x^2-(x_0+\mu z)^2}\right| \quad (19)$$

Integration of (18) with respect to x leads to logarithmic divergence and reproduces (5). Integration of the second term doubles that contribution. The energy flux (18) is shown in Figure 1. Near the discontinuity it decays proportionally to $1/\lambda$, where λ is the distance from the discontinuity.

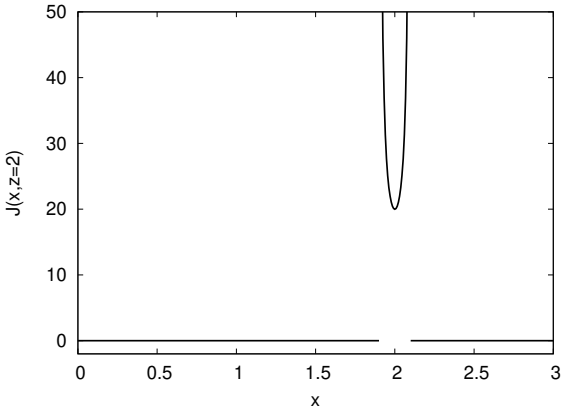

Figure 1: Vertical energy flux off a rectangular barrier of width $x_0=0.1$ in the WTA as a function of horizontal distance from the barrier, eq. (18). Near the two discontinuities at $x_d=z\pm x_0$, the flux is proportional to $1/|x-x_d|$.

2.3 Knife-edge to infinite order

The energy flux from an infinitely thin vertical barrier is tedious to obtain, as described in the appendix. To infinite order in slope, the streamfunction for the knife-edge topography is given by (40) for $x>0$ and $z>B$. The upward energy flux is (42). When integrated over all x, the total energy comes out to (6), as it must. The upward flux J depends on z, but for large z it has the simple form

$$J(x>0, z\gg B) = C\frac{\pi}{4}\frac{B^2}{\sqrt{\mu^2B^2-(\mu z-x)^2}} \quad (20)$$

That finally shows that a small distance λ from $x/\mu = z\pm B$, the singularity is of the form $1/\sqrt{\lambda}$.

Figure 2 shows the shape of (20). The two discontinuities correspond to the characteristics passing through

the tip of the knife-edge and through the tip of a vertically mirrored knife-edge, used to enforce the bottom boundary condition.

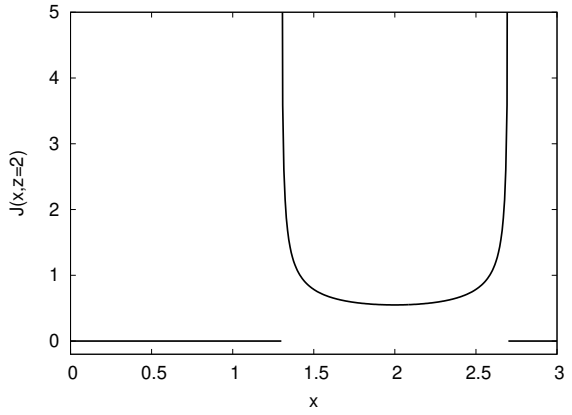

Figure 2: Vertical energy flux off a thin vertical barrier of height $B = 0.7$ as a function of horizontal distance from the barrier, based on an analytic solution that does not use the WTA (20). Near the two discontinuities at $x_d = z \pm B$, the flux is proportional to $1/\sqrt{|x - x_d|}$.

3 Regularization

The main result of the calculations above can be stated as follows. Singularities of the form as in Fig. 1 (with $x_0 \to 0$) should instead be of the form as in Fig. 2.

Neither $1/\lambda$ nor $1/\sqrt{\lambda}$ have an intrinsic length-scale. The smoothing length-scale, absent from the WTA but present in the full solution, is exactly μB. This is most easily interpreted in terms of slope rather than in terms of length. The effects of a discontinuity of height Δh are smeared out over a distance $\mu\Delta h$, i.e., the flux should be modified at supercritical slopes and locations shadowed by supercritical slopes. Since supercritical slopes are themselves shadowed, the latter subsumes the former.

To fix the WTA, a well-aimed limitation on the cumulative energy flux can be applied. The maximum increase in J over a distance $\mu\Delta h$ should not be more than for the knife-edge,

$$\int_x^{x+\mu\Delta h} dx' J(x', z) \lesssim \frac{\pi^2}{4} C(\Delta h)^2 \qquad \forall x \qquad (21)$$

where Δh is the maximum topographic relief over this distance,

$$\Delta h = \max_{\substack{x \le x_1 \le x+\mu\Delta h \\ x \le x_2 \le x+\mu\Delta h}} (|h(x_1) - h(x_2)|) \qquad (22)$$

The definition (22) is recursive. For a knife-edge it produces $\Delta h = B$ in every region shadowed by the knife-edge. For a straight segment of topography of slope $s < 1/\mu$ (subcritical) $\Delta h = 0$. For supercritical slopes, Δh spans supercritical regions and areas shadowed by them, exactly as desired.

Take a superposition of a continuous topography $h_1(x)$ and a discontinuous perturbation $h_2(x)$, then from (13) and the linearity of the Hilbert transform,

$$P[h_1 + h_2] = P[h_1] - 2C \int_{-\infty}^{\infty} dx h_2 \hat{H}'[h_1] + P[h_2] \quad (23)$$

The first term on the right-hand side converges, because h_1 is smooth. The cross-term also converges and only $P[h_2]$ diverges. Thus, regularization of $P[h_2]$ by itself regularizes a much more general situation. The statements on convergence can be proven using the Cauchy-Schwarz inequality and the equality $||\hat{H}[f]|| = \pi||f||$ for the L^2-norm [11], which shows that the integral in (23) is bounded from above by the variances of h_2 and h_1'.

To cure the WTA, the integration domain can be decomposed into segments D that are shadowed by supercritical topography and those that are not. The contribution from (one side of) a single-shadowed segment is

$$P_{\text{shadow}} = \min\left(C\frac{\pi^2}{4}(\Delta h)^2, \int_D dx J_{\text{WTA}}(x, 0)\right) \qquad (24)$$

The remainder of the integral is

$$P_{\text{purged}}[h] = \int_{\substack{-\infty \\ \text{without } D}}^{\infty} dx J_{\text{WTA}}(x, 0) = -C \int_{\substack{-\infty \\ \text{without } D}}^{\infty} dx h(x) \hat{H}'[h](x) \qquad (25)$$

The total power conversion is

$$P = P_{\text{purged}} + \sum_D P_{\text{shadow}} \qquad (26)$$

The sum is over all non-overlapping intervals D where h is shadowed by supercritical topography. The knife-edge has two such intervals. If the topography is subcritical everywhere, then D is empty and there is no modification to the WTA.

The prefactor $\pi^2/4$ in (24) is specific to the knife-edge. Solutions for a triangularly-shaped supercritical seamount [12], when applied to the infinite-depth ocean, show that the power conversion for triangular shape is lower than but similar to that of the knife-edge.

This specific procedure for regularization relies on the fact that the flux can be evaluated locally by $hH'[h]$, and it does not correspond to a single wavenumber cutoff in (3).

4 Numerical Example: Mid-Atlantic Ridge

Application of the formulas to a section of the mid-atlantic ridge serves as an illustration. Seafloor topography is at nominal $1'$ resolution (http://topex.ucsd.edu/WWW_html/mar_topo.html). The sample interval stretches from 70°W to 15°W at 25°N. Figure 3 shows a section of this west-east topographic transect and the associated energy flux evaluated with (16). The local contribution to the energy flux is particularly large where the topography is shadowed.

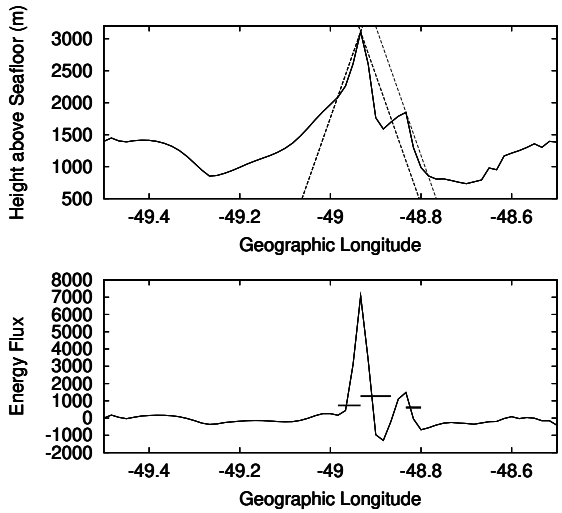

Figure 3: a) Topographic transect along 25° latitude in the Atlantic ocean, shifted vertically by 6 km. The horizontal interval spans about 100 km. The dashed lines indicate a critical slope of 20% that shadows segments of the topography. b) Vertical energy flux in arbitrary units evaluated with eq. (16). The thick horizontal lines represent flux limitations at shadowed segments of the topography based on the regularized WTA. The limitation is applied to the cumulative flux, such that the flux integrated over each of these segments is not allowed to exceed these mean values.

In calculating this expression, we have to deal with another logarithmic divergence in P_{WTA}, which arises because the topography does not level off at equal depth on both sides of the seamount. However, this divergence disappears when correction for finite ocean depth is applied [7, 2]. Here, it is eliminated by setting the depth outside of an interval of interest to 6000 m. Moreover, to eliminate end effects the entire topography is shifted by the same depth, such that $h(x)$ is ultimately padded by zeros on both sides.

To illustrate the main problem, we can evaluate P_{WTA} at various spatial resolutions, by smoothing the topography using a box filter. The solid line in Figure 4 shows P_{WTA} for spatial resolutions of $32'$ to $1'$ in geographic longitude. It shows a logarithmic increase, which demonstrates that calculating power conversion for real seafloor topography indeed suffers from the divergence problem, in agreement with earlier results [2, 3].

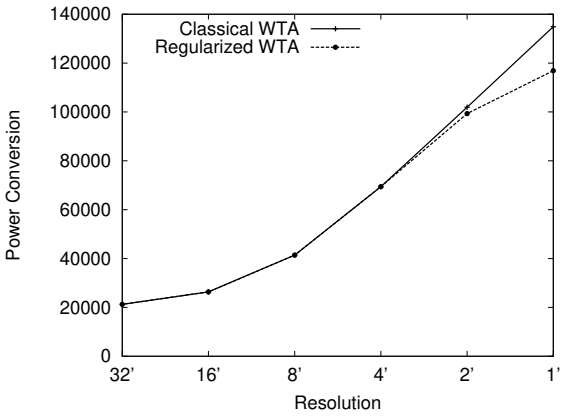

Figure 4: The solid line shows the logarithmic divergence of P_{WTA} with increasingly finer resolution. The dashed line represents power conversion according to the regularized WTA (24), (25), (26). The units of resolution are minutes of geographic longitude. At a resolution of $4'$ or coarser, there are no supercritical slopes.

The critical slope is set to an arbitrary but reasonable value of 0.2. The dashed line in Fig. 4 shows the power conversion obtained with the regularized WTA (24)–(26). Supercritical slopes start to appear at a resolution of $2'$. At the highest resolution ($1'$), the regularized WTA yields a power conversion that is 16% lower than the WTA. It is apparent from its definition that the regularized WTA approaches a finite limit as the resolution becomes infinitely fine. Figure 3b illustrates the local flux limitations.

5 Conclusions and Discussion

The lowest order solution (WTA) for an idealized model of the generation of internal gravity waves in the deep ocean diverges when the topography contains a discontinuity but higher order solutions are known to converge.

The length-scale of the singularity is determined for an infinitely thin vertical barrier where the infinite-order solution is known analytically. The vertical energy flux decays as $1/\sqrt{x}$, where x is the distance from the discontinuity. The length-scale of the divergent contribution spans exactly the width of topography shadowed by the wavebeam. For comparison, the same length scale in the WTA is zero, and when widened by introducing a thickness to the barrier, the flux is of the non-integrable form $1/x$.

The singular perturbation expansion can be regularized. Contributions to the WTA energy flux at shadowed segments of the topography should be limited by an upper bound motivated by the knife-edge solution (24)–(26), (11). The proposed modification of the WTA yields exactly the same result as the classical WTA for all subcritical topographies and it replicates the exact solution for the knife-edge topography. It surgically removes exaggerated flux contributions from an appropriately defined local flux (16), (11) and replaces it with a well-motivated expression that depends on topographic relief (24).

This regularization of the WTA makes it insensitive to small-scale topographic roughness, leading to robustness and increased accuracy even for continuous topography. When applied to a sample of seafloor topography, the WTA is found to indeed diverge logarithmically and the regularized WTA eliminates this divergence and leads to a decrease in the estimated power conversion.

For practical applications, variable stratification, corrections for finite ocean depth, and extension to quasi-3D need to be introduced, but because of the semi-local nature of the approximation, the nature of the singularity for a ridge is likely the same.

Both the results here and earlier analysis [2] suggest that there is still significant activity at the $1'$ (2 km) horizontal scale. Unless there is another physically motivated cutoff at larger scales, the power conversion has not yet converged even at $1'$ horizontal resolution. Thus, additional efforts to better quantify UV contributions are needed.

A Closed-form Expression for Streamfunction of Knife-Edge Topography

Llewellyn-Smith and Young [7] obtained the streamfunction for a knife-edge topography, using a Green's function approach [13]. They use the pressure along the knife-edge to calculate the power conversion, circumventing the need to explicitly obtain all of the streamfunction. Explicit expression for the streamfunction and the energy flux are derived here. Within this appendix $\mu = 1$ for convenience. The horizontal distance from the barrier is indicated with x, z is height above seafloor, and B denotes the height of the barrier.

Following Ref. [8], the real and imaginary part of the Green's function are

$$G_r(x,z,z') = \frac{1}{4}\left[-\Pi\left(\frac{x}{2(z-z')}\right) + \Pi\left(\frac{x}{2(z+z')}\right)\right] \tag{27}$$

$$G_i(x,z,z') = \frac{1}{4\pi}\ln\frac{|x+z-z'||x-z+z'|}{|x+z+z'||x-z-z'|} \tag{28}$$

where Π is the boxcar function, $\Pi(x) = 1$ for $|x| < 1/2$ and zero otherwise. The streamfunction is given by

$$\varphi(x,z) = \int_0^B dz'\gamma(z')(G_r(x,z,z') + iG_i(x,z,z')) \tag{29}$$

with

$$\gamma(z') = 2i\sqrt{\frac{1-\cos z'}{\cos z' - \cos B}} \approx 2i\frac{z'}{\sqrt{B^2 - z'^2}} =: i\tilde{\gamma} \tag{30}$$

where the expansion is for $B \ll \pi/2$. We are only interested in $z > B$ and, due to the symmetry of the streamfunction we can restrict ourselves to $x > 0$.

The imaginary part of the streamfunction is obtained from the real part of the Green's function,

$$\int_0^B dz'\tilde{\gamma}(z')G_r(x,z,z') = \frac{1}{4}\int_{|z-x|}^B dz'\frac{2z'}{\sqrt{B^2 - z'^2}} = \frac{1}{2}\sqrt{B^2 - (z-x)^2} \tag{31}$$

and it is zero for $|z - x| > B$.

The real part of the streamfunction is obtained separately for four spatial intervals,

1. For $0 < x < z - B$

$$\int_0^B dz'\tilde{\gamma}(z')G_i(z') = \frac{1}{2}\left(\sqrt{-B^2 + (x-z)^2} - 2z + \sqrt{-B^2 + (x+z)^2}\right) \qquad \text{for} \quad 0 < x < z - B \tag{32}$$

2. Now we evaluate the integral $\int_0^B dz'\tilde{\gamma}(z')G_i(z')$ for $z-B<x<z$, which is singular at $z'=z-x$. The non-singular part of the integral is

$$\begin{aligned}\int_0^B dz'\tilde{\gamma}(z')\ln\frac{|x+z-z'|}{|x-z-z'||x+z+z'|} &= 2B-2B\ln(z-x)+\pi\left(x+3z-2\sqrt{(x+z)^2-B^2}\right)\\ &\quad +2\sqrt{B^2-(x-z)^2}\ln\frac{z-x}{B+\sqrt{B^2-(x-z)^2}}\end{aligned} \tag{33}$$

The singular part of the integral is obtained by integrating from 0 to $\lim_{z'\to(z-x)^-}$ and from $\lim_{z'\to(z-x)^+}$ to $\lim_{z'\to B}$.

$$\int_0^B dz'\tilde{\gamma}(z')\ln|x-z+z'| = -2B+\pi(z-x)+2B\ln(z-x)+2\sqrt{B^2-(x-z)^2}\ln\frac{B+\sqrt{B^2-(x-z)^2}}{z-x} \tag{34}$$

The sum of (33) and (34) divided by 4π is

$$\int_0^B dz'\tilde{\gamma}(z')G_i(x,z,z') = z-\frac{1}{2}\sqrt{(x+z)^2-B^2} \qquad \text{for} \quad z-B<x<z \tag{35}$$

3. Now we evaluate the integral $\int_0^B dz'\tilde{\gamma}(z')G_i(z')$ for $z>x>z+B$, which is singular at $z'=x-z$. The non-singular part of the integral is

$$\begin{aligned}\int_0^B dz'\tilde{\gamma}(z')\ln\frac{|x+z-z'||x-z+z'|}{|x+z+z'|} &= -2B+\pi\left(x+3z-2\sqrt{(x+z)^2-B^2}\right)+2B\ln(x-z)+\\ &\quad 2\sqrt{B^2-(x-z)^2}\ln\frac{B+\sqrt{B^2-(x-z)^2}}{x-z}\end{aligned} \tag{36}$$

The negative of the singular part is

$$\int_0^B dz'\tilde{\gamma}(z')\ln|x-z-z'| = -2B+\pi(x-z)+2B\ln(x-z)+2\sqrt{B^2-(x-z)^2}\ln\frac{B+\sqrt{B^2-(x-z)^2}}{x-z} \tag{37}$$

The total contribution for $z>x>z+B$ is

$$\int_0^B dz'\tilde{\gamma}(z')G_i(x,z,z') = z-\frac{1}{2}\sqrt{(x+z)^2-B^2} \tag{38}$$

This is exactly the same as (35).

4. For $x>z+B$

$$\int_0^B dz'\tilde{\gamma}(z')G_i(z') = \frac{1}{2}\left(-\sqrt{-B^2+(x-z)^2}-2z+\sqrt{-B^2+(x+z)^2}\right) \qquad \text{for} \quad x>z+B \tag{39}$$

The imaginary part of the streamfunction is (31) and the negative of the real part is given by (32), (35), (38) and (39). The result for the streamfunction is

$$\varphi(x,z) = -\frac{1}{2}\times\begin{cases}\sqrt{-B^2+(x-z)^2}-2z+\sqrt{-B^2+(x+z)^2} & 0<x<z-B\\ \left(2z-\sqrt{(x+z)^2-B^2}\right)-i\sqrt{B^2-(z-x)^2} & |z-x|<B\\ -\sqrt{-B^2+(x-z)^2}-2z+\sqrt{-B^2+(x+z)^2} & x>z+B\end{cases} \tag{40}$$

The derivative for $|x-z|<B$ is

$$\frac{\partial\varphi}{\partial z} = -1+\frac{1}{2}\frac{x+z}{\sqrt{(x+z)^2-B^2}}+\frac{i}{2}\frac{x-z}{\sqrt{B^2-(z-x)^2}} \qquad \text{for} \quad |x-z|<B \tag{41}$$

The time-averaged energy flux in the vertical direction (9) is

$$\begin{aligned} J(x,z) &= \pi C \Im(\varphi^* \varphi_z) \\ &= C\frac{\pi}{4}\left[\left(-2z+\sqrt{(x+z)^2-B^2}\right)\frac{x-z}{\sqrt{B^2-(z-x)^2}}+\sqrt{B^2-(z-x)^2}\left(2-\frac{x+z}{\sqrt{(x+z)^2-B^2}}\right)\right] \end{aligned} \quad (42)$$

for $|z-x|<B$, and it is zero for $|x-z|>B$.

The parameter μ can be reintroduced by replacing x with x/μ. The power in the wave beam is obtained by an integral over x,

$$\int_{z-B}^{z+B} dx J(x,z) = C\frac{\pi^2 B^2}{4} \quad (43)$$

The total power is twice as much due to the contribution from $x<0$, and thus agrees with (6).

References

[1] C. Garrett and E. Kunze, Annu. Rev. Fluid Mech. **39**, 57 (2007).

[2] J. Nycander, J. Geophys. Res. **110**, C10028 (2005).

[3] E. Di Lorenzo, W. R. Young, and S. G. Llewellyn-Smith, J. Phys. Oceanogr. **36**, 1072 (2006).

[4] P. G. Baines, J. Fluid Mech. **46**, 273 (1971).

[5] N. J. Balmforth, G. R. Ierley, and W. R. Young, J. Phys. Oceanogr. **32**, 2900 (2002).

[6] T. H. Bell, J. Fluid Mech. **67**, 705 (1975).

[7] S. G. Llewellyn-Smith and W. R. Young, J. Fluid Mech. **495**, 175 (2003).

[8] J. Nycander, J. Fluid Mech. **567**, 415 (2006).

[9] O. Buhler and C. J. Muller, J. Fluid Mech. **588**, 1 (2007).

[10] N. Schorghofer, Fluid Dyn. Res. **42**, 065503 (2010).

[11] F. W. King, *Hilbert Transforms: Volume 1* (Cambridge University Press, 2009).

[12] F. Petrelis, S. G. Llewellyn-Smith, and W. R. Young, J. Phys. Oceanogr. **36**, 1053 (2006).

[13] R. M. Robinson, Deep Sea Res. **16**, 421 (1969).